Inorganic Chemistry

ARTICLE

pubs.acs.org/IC

Water Exchange Reactivity and Stability of Cobalt Polyoxometalates under Catalytically Relevant pH Conditions: Insight into Water Oxidation Catalysis

Dominik Lieb, Achim Zahl, Elizabeth F. Wilson, Carsten Streb, Leanne C. Nye, Karsten Meyer, and Ivana Ivanović-Burmazović*

Department of Chemistry and Pharmacy, University of Erlangen—Nürnberg, Egerlandstr. 1, 91058 Erlangen, Germany

Supporting Information

ABSTRACT: Water exchange on a molecular, purely inorganic cobalt-based water oxidation catalyst, $[Co_4^{II}(H_2O)_2(\alpha\text{-}P_1W_9O_{34})_2]^{10-}$ (**1**), in the catalytically relevant pH region (pH 6−10) is studied using ^{17}O-NMR spectroscopy and ultrahigh-resolution electrospray ionization mass spectrometry. The results are compared with those of the inactive $[Co^{II}(H_2O)_1Si_1W_{11}O_{39}]^{6-}$ (**2**), which is stable in the same pH region. The results obtained provide mechanistic details of the elementary reaction step related to the water oxidation on homogeneous metal oxide catalysts under catalytically relevant conditions. It is shown that the structural integrity of **1** and **2** is maintained, no deprotonation of the aqua ligands on the Co(II) centers occurs, and the water exchange does not undergo any mechanistic changeover at the catalytic pH conditions. We have demonstrated that the water exchange process is influenced by the cluster environment surrounding the water binding sites and is fast enough to not be rate-limiting for the water oxidation catalysis.

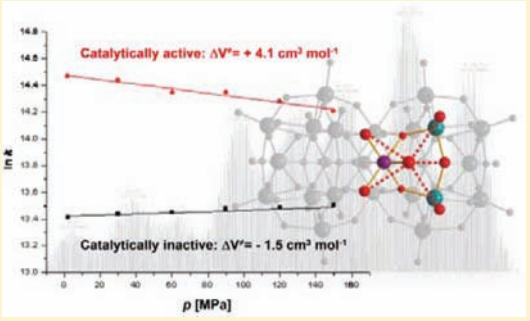

INTRODUCTION

The development of stable water oxidation catalysts[1−3] (WOCs) has been driven by a variety of chemical approaches, ranging from solid-state heterogeneous systems[4−6] to molecular, homogeneous WOCs.[2,7−10] Much attention has been paid to the bottom-up design of molecular WOCs, as they allow facile chemical tuning as well as better experimental access to investigate the underlying catalytic mechanisms. This mechanistic understanding is crucial as it forms the basis for the development of high efficiency WOC systems. To date, the main challenges which impede WOC development are the harsh reaction conditions which demand high thermal, hydrolytic, and oxidative stability under catalytic conditions. This is particularly problematic for coordination-compound-based WOCs where the organic ligands are prone to oxidative degradation, caused by the formation of reactive oxygen species (ROS). Recently, Hill et al. reported an all-inorganic WOC, $[Co^{II}_4(H_2O)_2(\alpha\text{-}P_1W_9O_{34})_2]^{10-}$ (**1**),[11,12] where a catalytically active $\{Co_4\}$ core is stabilized by two lacunary $[\alpha\text{-}P_1W_9O_{34}]$ phosphotungstate shells. Importantly, it was shown that this molecular catalyst can oxidize water at pH 7.5−8 (with maximum activity observed at pH 8) using $[Ru(bipy)_3]^{3+}$ as the stoichiometric electron acceptor (see Scheme), whereas at pH 6.2 no catalytic activity was observed.[11] Additionally, the optimal photocatalytic performance of **1** in light-driven water oxidation is achieved at pH 8.[12]

For all WOCs, coordination of water to a redox-active metal center is a precondition for its activation toward the electron transfer process (so-called metal ion coupled electron transfer[13]). In the structure of WOC **1**, there are two equivalent water binding sites, located on two peripheral Co centers on opposite sides of the cluster, see Figure 1. It is proposed that these two water binding sites, in combination with the redox activity of the Co(II) centers, enable the efficient catalytic oxidation of water to molecular oxygen. It is therefore of vital importance to investigate and establish the underlying kinetics of the water exchange at the cobalt centers so as to better understand and control the overall catalytic mechanism.

This report investigates the water exchange on the cobalt centers in **1** in the pH region from 6 to 10 (around its maximum catalytic activity observed at pH 8) to gain insight into the elementary reaction steps involved in the overall water oxidation process. In order to compare these findings with an inactive but structurally related cobalt system, experiments were conducted using the inactive compound $[Co^{II}(H_2O)_1Si_1W_{11}O_{39}]^{6-}$ (**2**) as a reference material, which is reported to be stable in the same pH range as the active compound **1**.[11] The kinetic parameters of the water exchange reactions were determined using temperature- and pressure-dependent ^{17}O-NMR spectroscopy in aqueous solutions at

Received: June 10, 2011
Published: August 02, 2011

Scheme 1. Homogeneous Water Oxidation Catalyzed by 1[11]

$$4[Ru(bipy)_3]^{3+} + 2H_2O \xrightarrow{1} 4[Ru(bipy)_3]^{2+} + 4H^+ + O_2$$

pH 6.1, 8, and 10. The solutions were further analyzed using ESI-MS to investigate and verify the structural integrity of **1** and **2** in the pH range 5−10.

EXPERIMENTAL SECTION

General Remarks. All chemicals were purchased from Sigma Aldrich or ACROS and were of reagent grade. The chemicals were used without further purification unless stated otherwise. Syntheses of **1** and **2** have been performed as described in the literature.[11,14] For experimental details, see the Supporting Information.

FT-IR Spectroscopy. FT-IR spectroscopy was performed on a Shimadzu FT-IR-8400S spectrometer. Samples were prepared as KBr pellets.

UV−Vis Spectroscopy. UV−vis spectroscopy was performed on a Shimadzu UV-2401PC spectrophotometer or a Varian Cary 50 spectrophotometer. Compounds **1** and **2** were investigated at pH 5, 8, and 10 (Figures S3 and S4, Supporting Information).

^{17}O NMR Spectroscopy. For the ^{17}O-NMR water exchange measurements, 10% enriched ^{17}O-labeled water (D-Chem Ltd. Tel Aviv, Israel) was used. The polyoxometalate samples were prepared by dissolved weighed amounts of the complex and an appropriate buffer solution (HEPES buffer for measurement at pH 8, CAPS buffer at pH 10, and PIPES buffer at pH 6.1). These buffers were chosen, because they are noncoordinating and therefore do not interfere in the ^{17}O-NMR dependent measurements. Their pK_a values are not pressure- and temperature-dependent.[15] The resulting solution was transferred to the NMR tube under an argon atmosphere. The pH was determined in the NMR tube using a micro-pH meter, Innovative Instruments, Inc. The concentrations of the complexes were either 8 or 10 mM for $Na_{10}[Co_4(H_2O)_2(PW_9O_{34})_2]$ (**1**) and 25 mM for $K_6[Co(H_2O)SiW_{11}O_{39}]$ (**2**).

Variable-temperature/-pressure Fourier-transform ^{17}O-NMR spectra were recorded at a frequency of 54.24 MHz and at a magnetic induction of 9.4 T on a Bruker Advance DRX 400WB spectrometer equipped with a superconducting BC-94/89 magnet system. The temperature dependence of the ^{17}O-line broadening was studied over the temperature range 278.2−338.2. K for compound **1** and in the range of 274.2−368.2 K for compound **2**. A homemade high-pressure probe described in the literature[16] was used for the variable-pressure experiments, which were conducted at the selected temperature and at ambient, 2, 30, 60, 90, 120, and 150 MPa pressures. A standard 5 mm NMR tube cut to a length of 50 mm was used for the sample solutions. The pressure was transmitted by a movable macor piston, and the temperature was controlled as described elsewhere.[16]

For all measurements, reference spectra from the pure solvent without POM (i.e., blank buffer at pH 6.1, pH 8, or pH 10) were first recorded to subtract the influence of the solvent surrounding the water exchange. Afterward, the sample was prepared in the measured blank buffer solution.

Mass Spectrometry. High mass accuracy ESI spectra were recorded on an ultrahigh-resolution ESI-Time-Of-Flight MS, a Bruker Daltoniks (Bremen, Germany) maXis. Spectra were obtained in negative-ion mode, with the capillary held at 4000 V. The drying gas flow rate was 7.0 L min^{-1} with a temperature of 240 °C. The nebulizer gas was at a pressure of 30.5 psi/2 bar. The m/z range detected was from 100 to 2000. A calibration tune mix (Agilent Technologies) was sprayed immediately prior to analysis to ensure a high mass accuracy to assist in the identification of peaks. The flow rate of the solutions was 300 μL/h. The POMs were dissolved in either H_2O or a H_2O/MeCN mixture (80:20) to improve peak intensity.

Peaks were identified with the aid of the simulated isotopic patterns created within the Bruker Data Analysis software. Peaks in spectra obtained in the H_2O/MeCN mixture were compared with the pure water spectra to ensure the slight solvent change had no effect on the peak masses or intensities. The sample concentrations for **1** and **2** were 1 mM.

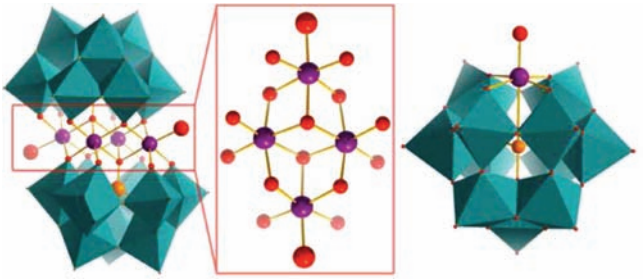

Figure 1. Left: Polyhedral representation of the water oxidation catalyst **1**. Center: Top view of the central $\{Co_4\}$ unit, highlighting the two water ligands (large red spheres). Right: Polyhedral representation of the inactive species **2**. Color scheme: $\{WO_6\}$, green; Co, purple; O, small red spheres; H_2O, large red spheres; P and Si, orange spheres.

RESULTS AND DISCUSSION

Until recently,[16] the water exchange on a Co(II) center has only been reported in the literature for the $[Co(H_2O)_6]^{2+}$ complex (the k_{ex}(298 K) values range from 1.35×10^6 to 3.18×10^6 s^{-1}, $\Delta S^{\ddagger}$ from −17 to +44 J K^{-1} mol^{-1}, and $\Delta H^{\ddagger}$ from 33.4 to 49.7 kJ mol^{-1}, whereas for $\Delta V^{\ddagger}$, only one value of +6.1 ± 0.2 cm^3 mol^{-1} is available in the literature).[18] More data are available for Co(III) complexes where the rate of water exchange varies from 10^{-6} s^{-1} to 10^2 s^{-1}, thus confirming the substitution inertness of Co(III).[19,20] Due to this profound difference in substitution behavior, water exchange measurements can be used as a molecular probe to determine the redox state of cobalt centers in aqueous solution. It is obvious that the substitution lability of the Co(II) centers is vital for fast kinetics on any cobalt catalyzed water oxidation process and at the same time makes a Co(II) form of WOCs critical in terms of catalyst stability within the overall catalytic cycle. With this in mind, examination of the structure of **1** shows that the supporting $\{PW_9\}$ units lend rigidity to the catalyst and provide a degree of stabilization to the generally labile Co(II) species. In addition, **1** can be considered an ideal molecular model for well-known heterogeneous cobalt phosphate WOCs,[5] and a better understanding of the water exchange mechanism of **1** might help to understand the activity of heterogeneous Co-based WOCs.

On the basis of previous studies,[21] one would expect that the coordination of negatively charged oxo ligands and the high overall negative charge in **1** should enhance the reactivity of the Co−OH_2 moiety and result in a considerably higher exchange rate k_{ex} as compared with the native $[Co(H_2O)_6]^{2+}$ complex. However, interestingly, in a recent study, Casey et al. have shown that the rate constants for the water exchange on **1**, at pH's 4.6, 5.4, and 6, and catalytically inactive $[Co^{II}_4(H_2O)_2(P_2W_{15}O_{56})_2]^{16-}$, at pH values 4.5, 5.4, and 6.3, are comparable with the reported values for $[Co(H_2O)_6]^{2+}$ (Table 1), with the polyoxometalates remaining intact under

dx.doi.org/10.1021/ic201243n |*Inorg. Chem.* 2011, 50, 9053–9058

Table 1. Water Exchange Parameters for 1, 2, and $[Co(H_2O)]^{2+}$ Determined at Different pH Values Using Temperature and Pressure Dependent ^{17}O-NMR Spectroscopy (For Details, See the Supporting Information)

compound	pH	k_{ex} [s^{-1}][a]	$\Delta H^{\ddagger}$ [kJ mol^{-1}]	$\Delta S^{\ddagger}$ [J mol^{-1} K^{-1}]	$\Delta V^{\ddagger}$ [cm^3 mol^{-1}]	ref
1	10.0[b]	$2.20 \pm 0.11 \times 10^6$	23.4 ± 1.1	-45.0 ± 3.7	n.d.	this work
1	8.0[c]	$1.92 \pm 0.13 \times 10^6$	23.0 ± 0.4	-47.5 ± 1.2	$+4.1 \pm 0.5$[d]	this work
1	6.1[e]	$1.99 \pm 0.11 \times 10^6$	23.3 ± 0.7	-46.2 ± 2.3	n.d.	this work
1	6.0[f]	$1.50 \pm 0.20 \times 10^6$	24.6 ± 0.2	-44.3 ± 0.6	n.d.	17
1	5.4[f]	$1.55 \pm 0.30 \times 10^6$	39.8 ± 0.3	$+7.1 \pm 1.2$	$+5.6 \pm 1.6$	17
1	4.6[f]	$1.75 \pm 0.20 \times 10^6$	35.5 ± 0.2	-6.4 ± 0.6	n.d.	17
2	10.0[b]	$1.34 \pm 0.10 \times 10^5$	45.8 ± 1.1	$+6.8 \pm 3.5$	n.d.	this work
2	8.0[c]	$1.84 \pm 0.23 \times 10^5$	40.3 ± 2.2	-8.9 ± 6.7	-1.5 ± 0.2[g]	this work
2	6.1[h]	$1.65 \pm 0.16 \times 10^5$	37.8 ± 1.8	-18.6 ± 5.6	n.d.	this work
$[Co(H_2O)_6]^{2+}$	~1.0	1.35 ± 10^6	33.4	-17.1	n.d.	19
$[Co(H_2O)_6]^{2+}$	~1.0	3.18 ± 0.17 x10^6	46.9 ± 1.2	$+37.2 \pm 3.7$	$+6.1 \pm 0.2$	18

[a] At 298.2 K. [b] 0.2 M CAPS buffer. [c] 0.2 M HEPES buffer. [d] Measured at 293.2 K. [e] 0.11 M PIPES buffer. [f] Without buffer. [g] Measured at 328.2 K. [h] 0.2 M PIPES buffer.

these pH conditions.[17] It should, however, be stressed that in these slightly acidic solutions no catalytic activity was observed for **1**.[11] Therefore, the goal of this work is to shed light on the solution behavior of **1** under catalytically relevant pH conditions, in particular at pH 8, as the maximum catalytic activity was observed at this pH value for both dark-[11]and light-driven[12] water oxidation.

In this work, ^{17}O-NMR spectroscopic investigations of the water exchange on **1** have shown that the rate constant at catalytic pH, i.e., pH 8, is also comparable with that for $[Co(H_2O)_6]^{2+}$ (Table 1). In order to clarify the pH-dependent speciation of **1**, we also performed kinetic studies at pH 6.1 and 10. The obtained values for k_{ex} and corresponding activation parameters do not change significantly over the pH range measured (Table 1), suggesting that the coordinated water molecules do not undergo deprotonation in the pH range 4.6−10. This is supported by the single-crystal X-ray structure of **1**, previous observations by Hill et al.,[11] and, additionally, by our UV−vis and ultrahigh-resolution (UHR) electrospray ionization mass spectrometry (ESI-MS) measurements at pH 5, 8, and 10 (see Supporting Information). Variable pressure ^{17}O-NMR spectroscopy allowed us to gain more insight into the exchange mechanism, and the data analysis (Figure 2, left) suggested an interchange mechanism with a slightly dissociative character, based on the activation volume, $\Delta V^{\ddagger}$, see Table 1.

Structural analysis of the average Co−OH_2 bond distances (d_{Co-O} = 2.116(6) Å in **1**[17] and ≤2.085 Å in $[Co(H_2O)_6]^{2+}$)[21,22] indicates that the oxo ligands in **1** have a weakening effect on the Co−OH_2 bond; however, our results show that this feature is not reflected by a significantly increased water exchange rate in **1** when compared with $[Co(H_2O)_6]^{2+}$ (Table 1). One possible explanation would be the stabilization of the water ligand in **1** through cluster-based hydrogen-bonding interactions. These could be formed by the protonation of oxo ligands which surround the coordinated water ligand in the binding site of **1**, hence decreasing the rate of the water exchange. Analysis of the reported crystal structure of **1** supports this hypothesis, as the cluster environment surrounding the catalytic binding site has the geometry required to promote such stabilization, see Figure S1 (Supporting Information).

In order to investigate this hypothesis, and to provide direct mass spectrometric confirmation that **1** remains intact and does not undergo deprotonation of the coordinated water molecules in the studied pH range, we used the technique of UHR-ESI-MS. In previous studies, electrospray and cryospray mass spectrometric techniques have been shown to allow efficient transfer of a range of intact POM clusters from the solution state into the gas phase for detection using high-resolution time-of-flight detectors.[25−27] Analysis of the spectra demonstrates that the main metal oxide units of the cluster remain intact in solution, as evidenced by the base peak at m/z 1202.6031 assigned as $[Co^{II}_4(PW_9O_{34})_2H_1Na_5]^{4-}$ (Figure 3). We are also able to observe ions from this cluster which have maintained the coordination of one of the two water ligands, e.g., $[Co^{II}_4(PW_9O_{34})_2(H_2O)_1H_4Na_1]^{5-}$ at m/z 947.8896 (Table 2).

The peak assignments of **1** are supported in three ways: First, the measurements were recorded at the high mass accuracy and resolution afforded by our instrument; for example, the base peak at m/z 1202.6031 has a mass accuracy of −0.08 ppm with the difference between the central peak in the measured and simulated isotopic envelopes being only 0.0001 Da. Second, assignments were supported from a visual comparison of the isotopic envelopes. Third, assignments were supported from the observation of a series of peaks, e.g., peaks with the same charge where a proton has replaced a sodium ion as a counterion. This switching of counterions was also observed to correlate with the peaks where a water molecule was retained by intact compound **1**: peaks with a greater number of protons as counterions were more likely to retain a water molecule. This confirms the observations from the ^{17}O-NMR experiments and, as mentioned previously, indicates that protons bound to the oxo ligands of the cluster adjacent to the active cobalt centers are stabilizing the water molecules and therefore making their exchange rates slower than what would be expected (*vide supra*). The results obtained at pH 5, 8, and 10 confirm the existence of the same species. At pH 5, increased numbers of species are detected where more of the sodium counterions have been replaced by protons compared with pH 8 and 10 (see Supporting Information, Figure S40 and S41).

It should be noted at this point that, although it is generally known that polyoxometalate structures decompose under basic

dx.doi.org/10.1021/ic201243n |*Inorg. Chem.* 2011, 50, 9053–9058

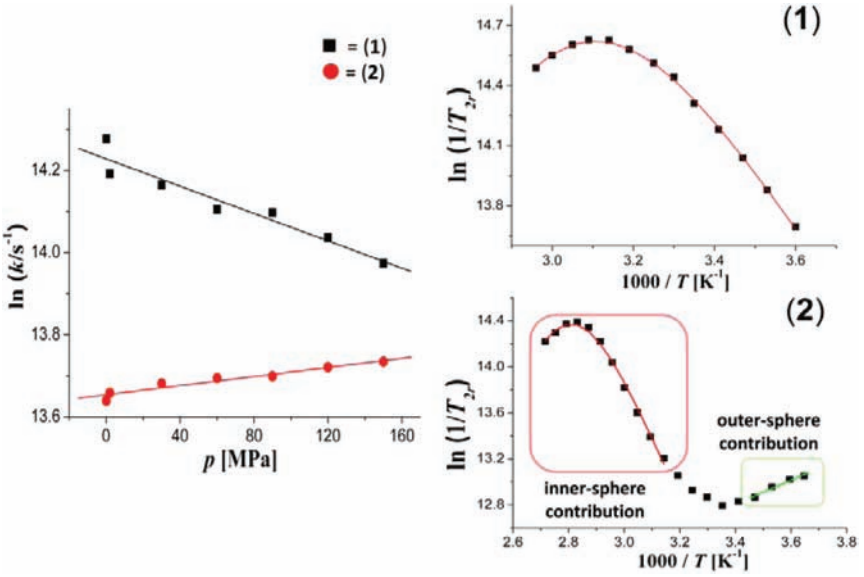

Figure 2. Pressure (left) and temperature (right) dependence of the water exchange on **1** (top) and **2** (bottom) as determined by ^{17}O-NMR spectroscopy in an aqueous buffer solution at pH 8 (see Supporting Information for details).

Table 2. UHR-ESI-MS Data at pH 8 Showing the Intact Cluster of 1 (m/z Values Are Reported for Central Peak in Isotopic Envelope, see Supporting Information for Spectra)

recorded m/z	calculated m/z	peak assignment
943.4921	943.5013	$[Co^{II}_4(PW_9O_{34})_2(H_2O)H_5]^{5-}$
947.8896	947.8977	$[Co^{II}_4(PW_9O_{34})_2(H_2O)H_4Na]^{5-}$
957.4868	957.4847	$[Co^{II}_4(PW_9O_{34})_2(H_2O)HNa_4]^{5-}$
1202.6031	1202.6032	$[Co^{II}_4(PW_9O_{34})_2HNa_5]^{4-}$
1208.1001	1208.0987	$[Co^{II}_4(PW_9O_{34})_2Na_6]^{4-}$
1618.4668	1618.4614	$[Co^{II}_4(PW_9O_{34})_2Na_7]^{3-}$

conditions, the above work using compound **1** has illustrated this cluster's stability over the pH range of study, i.e., between pH 5 and 10. In order to then compare **1** with an inactive cobalt cluster which is also stable in this pH range, the stability of **2** was carefully checked, in particular, at pH 10, to ensure that cluster integrity is retained at this level of basicity. It was found that even boiling compound **2** for 30 min in a pH 10 solution gave the same mass spectra and UV/vis spectra as observed at lower pH values without any signs of decomposition. However, at pH 12, a rapid decomposition of compound **2** was observed (for spectra see Figure S42, Supporting Information). ^{17}O-NMR data of the sample at pH 10 were collected before and after performing the temperature dependent measurements, and no change in line width of the ^{17}O signal could be observed, indicating no release of free Co(II) or change in the chemical environment of the Co(II) center which would alter the transverse relaxation of the ^{17}O nucleus in compound **2** significantly.[17] Given this clear indication of the stability of **2** over the pH range 5−10, this compound was selected for comparison studies with **1**—hence, ^{17}O-NMR water exchange studies were conducted on **2**.

It was shown that water exchange on **2** is 1 order of magnitude slower as compared with **1** and $[Co(H_2O)_6]^{2+}$ and does not change significantly in the pH range from 6.1 to 10 (Table 1). The exchange mechanism has a less dissociative character than in **1** based on a small negative value of $\Delta V^{\ddagger}$ (Table 1). The reason

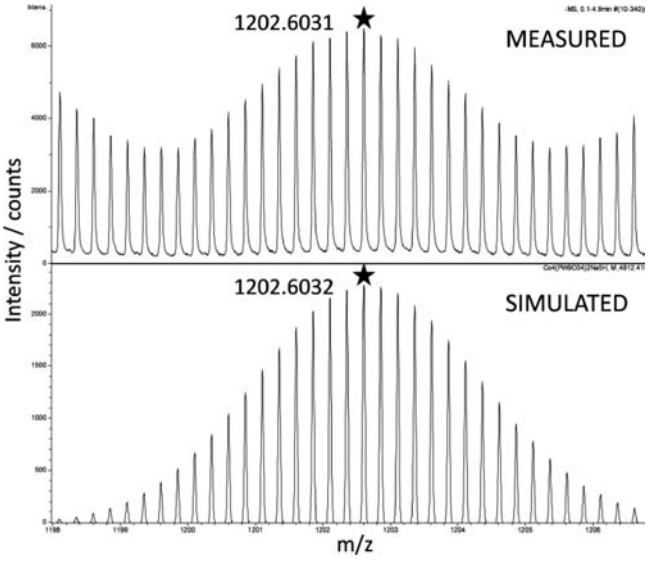

Figure 3. UHR-ESI-MS of **1** showing the isotopic envelope for $[Co^{II}_4(PW_9O_{34})_2HNa_5]^{4-}$ both measured and simulated.

for the slower exchange is a strongly elongated Co−O bond (2.3118(3) Å) *trans* to the water ligand, resulting in a *quasi*-five-coordinate environment (Figure 1), leading to a shortening of the Co−OH_2 bond.[28] This changes the water exchange into a more associative mechanism (Figure 2, left).

In contrast to structure **1**, the coordinated water ligand in **2** is exposed to the bulk solution with no additional interaction with the cluster shell (Figure 1 and Figure S2, Supporting Information). This structural difference in the water binding sites in **1** and **2** is also nicely reflected in the temperature dependencies of the reduced transverse relaxation rates ($1/T_{2r}$) given in Figure 2. The prominent contribution of an outer-sphere mechanism to this relaxation rate arises from long-range interactions of the unpaired electrons of the cobalt center with water

dx.doi.org/10.1021/ic201243n |*Inorg. Chem.* 2011, 50, 9053–9058

molecules of the outer coordination sphere. This is clearly visible by a changeover to a positive slope at low temperatures (Figure 2, bottom right) and is only possible in **2** where the cobalt center is sufficiently exposed to the bulk solution (Figure S2). In contrast, the water ligands in **1** are shielded by the cluster shells (Figure S2) and are protected from direct interactions with the bulk solution, therefore diminishing an outer-sphere contribution to T_{2r} (see Supporting Information).

The UV/vis spectra at pH 5, 8, and 10 demonstrate no change in protolytic speciation of **2** in this pH region (see Supporting Information). UHR-ESI-MS data for compound **2** at the same pH values demonstrate the stability of this cluster over this pH range, as the spectra show no decomposition and are almost identical. The peaks observed consist of the intact cluster, however, always with the loss of the Co-bound water ligand, e.g., $[(Co^{II}SiW_{11}O_{39})K_2H_2]^{2-}$ at m/z 1406.5596 (Table S12, Supporting Information). This is in contrast to the MS data for **1**, where coordinated water ligands are still observed in the mass spectra. Interestingly, there is also evidence of the formation of dimers, e.g., $[(Co^{II}SiW_{11}O_{39})_2K_6H]^{5-}$ at m/z 1140.2299 (Figures S29−S31, S35, and S37, Supporting Information), whereas such dimer formation was not observed for **1**. As with the monomeric units, the Co-bound water ligand was not observed attached to the dimers. As motioned above, the cobalt center in **2** is more exposed to the external environment (Figure 1 and Figure S2, Supporting Information) and thus is potentially more prone to dimerization than **1**. We can speculate that dimer formation results in the replacement of the terminal water ligand by an oxo ligand of the adjacent cluster as a result of the electrospray process.

CONCLUSION

In conclusion, we have shown that both clusters **1** and **2** are stable in the catalytically most relevant pH region of pH 6−10 where water oxidation is thermodynamically favored due to decreasing redox potentials at higher pH values. In addition, our results show that in this pH range, the coordination of water ligands on the Co centers is maintained, and no deprotonation (i.e., formation of Co−hydroxo or Co−oxo species) was observed. As a consequence, our results also demonstrate that the pK_a values for water molecules bound to Co(II) in **1** and **2** are above 10, which is higher than has been proposed for **1** by Casey et al. (pK_a ≈ 8).[17] We have demonstrated that the water exchange process on WOC **1** does not undergo any mechanistic changeover, and this process is faster and has a more dissociative character than that for inactive **2**, in the pH region of catalytic interest. However, as both the water exchange processes in **1** and **2** are much faster than the overall catalytic cycle (ca. 5 s^{-1}),[11] these steps cannot be rate-limiting and cannot, therefore, be responsible for the maximum catalytic activity at pH 8. Thus, most probably the electron transfer is the rate-limiting step, the tuning of which is crucial for the oxidation process. In general, at higher pH values, redox potentials are lower, favoring oxidation reactions. On the basis of these results, we can now suggest that the reason for the water oxidation capability of **1** is based first on its stability at higher pH values (pH > 7) and second on the specific binding mode of the water ligand to the Co center in the protected pocket-like active site of **1**. These two properties distinguish **1** from other Co−POMs tested thus far.[11] Further investigations of the pH dependence of cluster-based redox reactions are underway.

ASSOCIATED CONTENT

Supporting Information. Full experimental details, ^{17}O-NMR data treatment, and mass spectra of relevant peaks. This material is available free of charge via the Internet at http://pubs.acs.org.

AUTHOR INFORMATION

Corresponding Author

*Tel.: +49 9131 8525428. Fax: +49 9131 8527345. E-mail: ivana.ivanovic@chemie.uni-erlangen.de.

ACKNOWLEDGMENT

Financial support by the DFG (SFB 583), Fonds der Chemischen Industrie, and Alexander von Humboldt-Foundation are gratefully acknowledged.

REFERENCES

(1) Lewis, N. S.; Nocera, D. G. *Proc. Natl. Acad. Sci. U. S. A.* **2006**, *103*, 15729–15735.
(2) Yagi, M.; Kaneko, M. *Chem. Rev.* **2001**, *101*, 21–35.
(3) Bard, A. J.; Fox, M. A. *Acc. Chem. Res.* **1995**, *28*, 141–145.
(4) Khan, S. U. M.; Al-Shahry, M.; Ingler, W. B. *Science* **2002**, *297*, 2243–2245.
(5) Kanan, M. W; Nocera, D. G. *Science* **2008**, *321*, 1072–1075.
(6) Kudo, A.; Miseki, Y. *Chem. Soc. Rev.* **2009**, *38*, 253–278.
(7) Gilbert, J. A.; Eggleston, D. S.; Murphy, W. R.; Geselowitz, D. A.; Gersten, S. W.; Hodgson, D. J.; Meyer, T. J. *J. Am. Chem. Soc.* **1985**, *107*, 3855–3864.
(8) Sartorel, A.; Carraro, M.; Scorrano, G.; De Zorzi, R.; Geremia, S.; McDaniel, N. D.; Bernhard, S.; Bonchio, M. *J. Am. Chem. Soc.* **2008**, *130*, 5006–5007.
(9) Geletii, Y. V.; Huang, Z. Q.; Hou, Y.; Musaev, D. G.; Lian, T. Q.; Hill, C. L. *J. Am. Chem. Soc.* **2009**, *131*, 7522–7523.
(10) Blakemore, J. D.; Schley, N. D.; Balcells, D.; Hull, J. F.; Olack, G. W.; Incarvito, C. D.; Eisenstein, O.; Brudvig, G. W.; Crabtree, R. H. *J. Am. Chem. Soc.* **2010**, *132*, 16017–16029.
(11) Yin, Q. S.; Tan, J. M.; Besson, C.; Geletii, Y. V.; Musaev, D. G.; Kuznetsov, A. E.; Luo, Z.; Hardcastle, K. I.; Hill, C. L. *Science* **2010**, *328*, 342–345.
(12) Huang, Z. Q.; Luo, Z.; Geletii, Y. V.; Vickers, J. W.; Yin, Q.; Wu, D.; Ding, Y.; Song, J.; Musaev, D. G.; Hill, C. L.; Lian, T. Q. *J. Am. Chem. Soc.* **2011**, *133*, 2068–2071.
(13) Morimoto, Y.; Kotani, H.; Park, J.; Lee, Y.-M.; Nam, W.; Fukuzumi, S. *J. Am. Chem. Soc.* **2011**, *133*, 403–405.
(14) Weakly, T. J. R.; Malik, S. A. *J. Inorg. Nucl. Chem.* **1967**, *29*, 2935–2944.
(15) Kitamura, Y.; Itoh, T. *J. Solution Chem.* **1987**, *16*, 715. Goldberg, R. N.; Kishore, N.; Lennen, R. M. *J. Phys. Chem. Ref. Data* **2002**, *31*, 231–370.
(16) Zahl, A.; Neubrand, A.; Aygen, S.; van Eldik, R. *Rev. Sci. Instrum.* **1994**, *65*, 882–886.
(17) Ohlin, C. A.; Harley, S. J.; McAlpin, J. G.; Hocking, R. K.; Mercado, B. Q.; Johnson, R. L.; Villa, E. M.; Fidler, M. K.; Olmstead, M. M.; Spiccia, L.; Britt, R. D.; Casey, W. H. *Chem.—Eur. J.* **2011**, *17*, 4408–4417.
(18) Ducommun, Y.; Newman, K. E.; Merbach, A. E. *Inorg. Chem.* **1980**, *19*, 3696–3703.
(19) Swift, T. J.; Connick, R. E. *J. Chem. Phys.* **1962**, *37*, 307–320. **1964**, *41*, 2553–2554.
(20) Brasch, N. E.; Buckingham, D. A.; Clark, C. R.; Rogers, A. J. *Inorg. Chem.* **1998**, *37*, 4865–4871.
(21) Dadci, L.; Elias, H.; Frey, U.; Hornig, A.; Koelle, U.; Merbach, A. E.; Paulus, H.; Schneider, J. S. *Inorg. Chem.* **1995**, *34*, 306–315.

(22) Lieb, D.; Zahl, A.; Shubina, T. E.; Ivanovic-Burmazovic, I. *J. Am. Chem. Soc.* **2010**, *132*, 7282–7284.
(23) Liu, H.; Wang, J.; Jian, F.; Xiao, H. *J. Clust. Sci.* **2009**, *20*, 621–629.
(24) Jeremic, D. A.; Kaluderovic, G. N.; Gomez-Ruiz, S.; Brceski, I.; Kasalica, B.; Leovac, V. M. *Cryst. Growth Des.* **2010**, *10*, 559–563.
(25) Wilson, E. F.; Abbas, H.; Duncombe, B. J.; Streb, C.; Long, D.−L.; Cronin, L. *J. Am. Chem. Soc.* **2008**, *130*, 13876–13884.
(26) Miras, H. N.; Wilson, E. F.; Cronin, L. *Chem. Commun.* **2009**, *11*, 1297–1311 and the references contained therein.
(27) Ma, M. T.; Waters, T.; Beyer, K.; Palamarczuk, R.; Richardt, P. J. S.; O'Hair, R. A. J.; Wedd, A. G. *Inorg. Chem.* **2009**, *48*, 598–606.
(28) Rotzinger, F. P. *J. Am. Chem. Soc.* **1997**, *119*, 5230–5238.

NOTE ADDED AFTER ASAP PUBLICATION

Reference 17 was corrected on August 9, 2011.